energies

MDPI

Article

The Viscosity and Combustion Characteristics of Single-Droplet Water-Diesel Emulsion

Jonghan Won [1], Seung Wook Baek [1,*], Hyemin Kim [2,*] and Hookyung Lee [3]

[1] Department of Aerospace Engineering, Korea Advanced Institute of Science and Technology (KAIST), 291 Daehak-ro, Yuseong-gu, Daejeon 34141, Korea; won1402@kaist.ac.kr
[2] Department of Aeronautical & Mechanical Design Engineering, Korea National University of Transportation, Daehak-ro 50, Chungju 27469, Korea
[3] Corporate R&D Institute, Doosan Heavy Industries and Construction, Yongin 16858, Korea; hookyung.lee@doosan.com
* Correspondence: swbaek@kaist.ac.kr (S.W.B.); enok2695@ut.ac.kr (H.K.); Tel.: +82-42-350-3714 (S.W.B.); +82-43-841-5838 (H.K.)

Received: 13 February 2019; Accepted: 10 May 2019; Published: 22 May 2019

Abstract: Diesel fuel exhibits excellent combustion characteristics and stability. However, diesel use is becoming restricted because of its associated environmental problems. Fuel emulsification, which increases efficiency and reduces pollution, became the solution of environmental problem. In this study, five water:diesel emulsions with mass ratios (0.3, 0.6, 1.0, 1.2, and 1.5) via ultrasonication were synthesized with and without surfactant. The optimal water:diesel ratio (=1:1) of an emulsion containing the surfactant was found by analyzing fuel concentration, mixing time, and viscosity. The combustion characteristics of single-droplet optimal emulsions were studied through ignition delay, burning rate, and total droplet lifetime at high temperature (400–700 °C) and pressure (1–15 bar), and micro-explosion phenomenon was observed. Although the ignition delay of emulsion increased, the total lifetime of the emulsion droplet was lower than that of diesel under 5 bar, 600 °C condition.

Keywords: water-diesel emulsion; diesel; droplet; viscosity; combustion; micro-explosion

1. Introduction

Diesel engines are more efficient, durable, and reliable than gasoline engines. Today, however, diesel engines are subjected to strict emission regulations worldwide in terms of particulate matter (PM), nitrogen oxides (NOx), and carbon monoxide (CO), all of which compromise human health [1]. An alternative fuel of higher combustion efficiency associated with fewer emissions is required. Several candidate fuels are available, of which emulsions have gained particular attention. Water-in-oil (W/O) emulsions exhibit higher combustion efficiency, associated with fewer emissions, than conventional fuels [2–4]. Such improvements are rendered possible by micro-explosions ("puffing"). During combustion, water droplets in the fuel evaporate, and the vapor thus becomes pure fuel given the difference in boiling point between water and oil. Puffing is initiated when water vapor has accumulated to a certain level inside droplets. Puffing enhances droplet atomization and evaporation, and reduces emissions [5,6]. Moreover, the heat consumed to evaporate water reduces the flame temperature and suppresses the generation of thermal NOx. Previous studies showed that NOx and PM levels could be reduced by 40% and 35% respectively, without compromising engine performance [7].

Several researchers have explored fuel properties, particularly combustion characteristics. Jang and Kim [8] studied the surface tension, dynamic viscosity, and light absorbance of an n-dodecane emulsion fuel. Surface tension decreased and dynamic viscosity increased sharply as the n-dodecane level rose. Light absorbance varied by the transient conditions. Elsanusi et al. [9] explored the stability

and combustion characteristics of diesel-biodiesel blended emulsions under various engine operating conditions. A mixed surfactant (2% w/v of hydrophilic lipophilic balance [HLB] 8.25, formed by mixing Span 80 and Tween 80) served as the emulsifier. When the water concentration increased, the thermal efficiency and CO emissions also increased, but the exhaust gas temperature and NOx emissions decreased. Reham et al. [10] studied the stability, physical properties, performance, and emission characteristics of biofuel emulsions. Stability was affected by the surfactant used (particularly its HLB value) and emulsion type. Water increased the density, viscosity and cetane number but decreased heating capacity. Jeong and Lee [11] examined autoignition and micro-explosion of water/n-decane emulsion droplets under normal pressure at high temperature. When the distance between droplet arrays and the water concentration increased, the ignition delay and time required for complete combustion also increased. However, the viscosity and combustion characteristics of an emulsion droplet require further study; physicochemical status is affected by the temperature, mixing method, and water:oil weight ratio, rendering research outcomes inconsistent [12–15]. Here, the optimum water:diesel ratio and mixing conditions were defined via viscosity analysis. Viscosity was measured at 15, 30, and 60 °C, and the optimum emulsion concentration determined. Then, combustion of single-droplet fuel emulsions, optimized in terms of the water:fuel ratio, was studied at high temperatures (400–700 °C) and pressures (1–15 bar).

2. Experimental Apparatus

2.1. Preparation of Emulsion Fuel

Distilled water (OCI Inc., 94 Sogong-ro, Jung-gu, Seoul, Korea) and commercial diesel (GS Caltex, 508 Nonhyeon-ro, Gangnam-gu, Seoul, Korea) were used to create water-diesel emulsions. Water and diesel were mixed (10 g amounts) in five water:diesel (W:D) mass ratios (0.3, 0.6, 1.0, 1.2, and 1.5) via ultrasonication (Sonics & Materials Inc., 53 Church Hill Rd, Newtown, CT, USA) over 20 min with successive on/off periods of 5 s to prevent temperature rise. Surfactant must be added to stabilize emulsions prior to extended storage. Surfactants of HLB 4–6 are commonly added to W/O emulsions, and surfactants of HLB 8–18 to oil-in-water emulsions. Selection of an appropriate surfactant is essential [16]. The addition of two different surfactants improves mixing ability because the physicochemical properties change [17]. Here, both Span 80 (HLB 4.3) and Tween 20 (HLB 16.7) were added. The HLB value of the mixed surfactant was calculated as a mass ratio [18]:

$$HLB_{ST} = f_T * HLB_T + (1 - f_T) * HLB_S \quad (1)$$

where f_T is the mass fraction of Tween 20, and T and S indicate Tween 20 and Span 80, respectively. The surfactants were mixed by stirring at 1500 rpm for 10 min (appropriate for surfactants of HLB 8–16, as reported in previous studies [19,20]. An HLB 14 surfactant afforded the best performance at 0.2 wt%. Figure 1 shows the emulsion fuel before and after ultrasonication without surfactant. Fuels of W:D mass ratios 0.3 and 0.6 did not mix perfectly; two phases were apparent. However, emulsions of water concentrations equal to or greater than those of diesel mixed readily (i.e., fuels with W:D ratios of 1.0, 1.2, and 1.5). Phase separation of these emulsions was first observed at 5 h after production; thin diesel layers appeared on top.

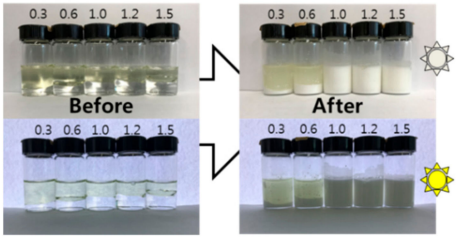

Figure 1. Emulsions viewed with and without backlighting before and after ultrasonication.

2.2. Viscosity Measurements

Viscosity is important during spray combustion; low-viscosity fuel affords superior atomization [21]. Viscosity was measured at ambient temperatures of 15, 30, and 60 °C. The rheometer (HAAKE RheoStress 6000, Thermo Fisher Scientific, Process Instruments, Karlsruhe, Germany) measured dynamic viscosity along the shear rate. All measurements were performed at least three times.

2.3. Constant-Volume Combustion Chamber

Figure 2 shows a schematic of the constant-volume combustion chamber [22]. An electric furnace maintained the ambient temperature within 400–700 °C using heating coils. The coils were surrounded by ceramic shields to protect against radiation. Each emulsion droplet (750 ± 100 μm) was suspended at the tip of a k-type thermocouple (a 50-μm-diamater Al-Cr wire). The mean droplet temperature measured by the thermocouple was at least 91% accurate in an earlier numerical simulation [23]. The electric furnace descended along two guides to the thermocouple; the droplet was thus instantly exposed to high temperature. Droplet evaporation and combustion were recorded by a high-speed camera (200 frames/s). Changes in droplet diameter were analyzed using Visual Basic software, as described previously [24,25]. Ambient temperature was controlled in the range 400–700 °C at intervals of 100 °C, with consideration of the boiling and autoignition points of diesel given as manufacturer (Table 1). Ambient pressure was controlled in the range 1–15 bar at intervals of 5 bar. All experiments were repeated at least five times.

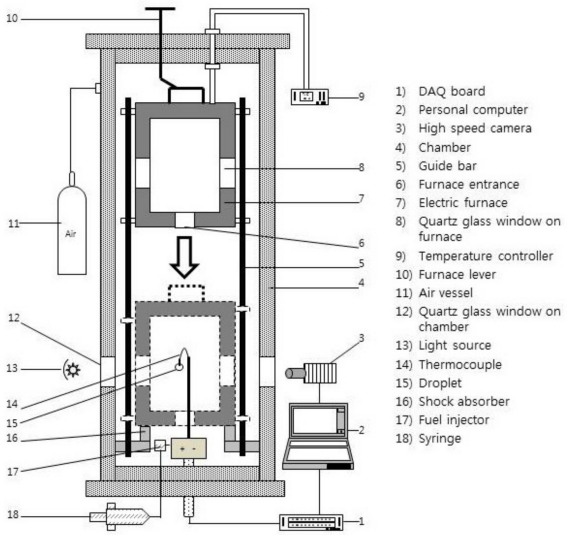

Figure 2. Schematic diagram of constant-volume combustion chamber used of Won et el. [22].

Table 1. The physicochemical properties of diesel.

Property	Diesel
Boiling point (°C)	130–360
Flash point (°C)	Higher than 40
Autoignition point (°C)	Higher than 260
Density at 15 °C (kg/m^3)	815–835
Cetane number	Higher than 52

3. Results

3.1. Viscosity of Emulsion Fuels

Generally, the viscosity of water and diesel remains uniform above a shear rate of 30 s^{-1}; both fluids exhibit Newtonian behavior [26]. Therefore, average viscosity was calculated after that shear

rate (at various temperatures) and compared to that of the reference [27] (Figure 3). The values for diesel differ by producer and thus cannot be readily compared to the reference values.

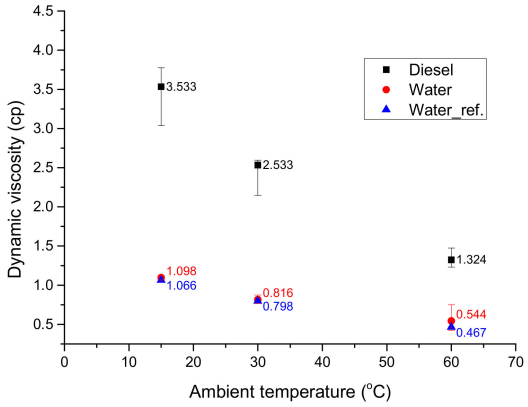

Figure 3. Viscosity of diesel and water at various temperatures.

Before measuring emulsion viscosity, it was necessary to establish an appropriate shear rate. Figure 4 shows that emulsion viscosity fell continuously as the shear rate rose; this is a representative feature of non-Newtonian fluid. The interfacial films surrounding droplets, which prevented them from coalescence, were destroyed at high shear rates. The emulsion viscosity then rapidly decreased because the water and diesel phases separated [28]. Between the shear rate of 40 and 100 s^{-1}, viscosity slowly changed, but only marginally. Thus, average viscosity was calculated at shear rates ranging from 40 to 100 s^{-1}.

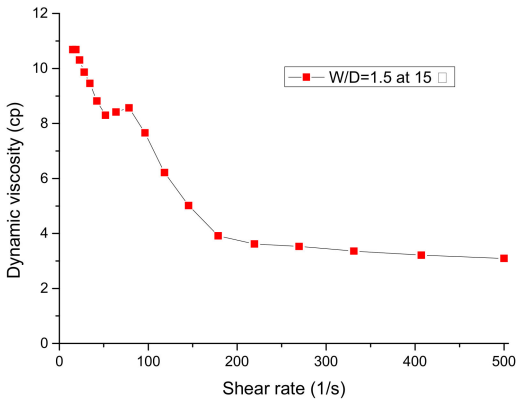

Figure 4. Viscosity changes of W:D = 1.5 emulsion as the shear rate rose at an ambient temperature of 15 °C.

Figure 5 shows the viscosity changes in the W:D = 1.0, 1.2, and 1.5 emulsions without surfactant at mixing times (operation times of ultrasonication) of 10 and 20 min. The W:D = 0.3 and 0.6 emulsions were not perfectly mixed; thus, they could not be measured the viscosity. Two-milliliter samples were extracted in mid-phase for measurements. The viscosity of the W:D = 1.0 emulsion was highest because dispersed droplet packing was maximal; the W:D = 1.5 emulsion exhibited the lowest viscosity because the droplet dispersion was lowest [28]. Generally, the viscosity/temperature curves of the W:D = 1.2 and 1.5 emulsions were exponential in shape. However, that of the W/D = 1.0 emulsion was not, because of rapid water droplet coalescence. As the temperature rose, the interfacial film first weakened and then broke; the dispersed water droplets then aggregated [29]. The W:D = 1.0 emulsion had a relatively large proportion of dispersed droplets; coalescence followed by separation of the water and diesel phases that occurred readily as the temperature rose. Viscosity changed markedly with mixing time for all emulsions. At a relatively low ambient temperature, 15 °C, the differences were not

large but increased greatly as the temperature rose. Thus, water and diesel were not uniformly mixed. As emulsion instability triggers combustion instability, surfactants must be added to ensure stability and uniformity.

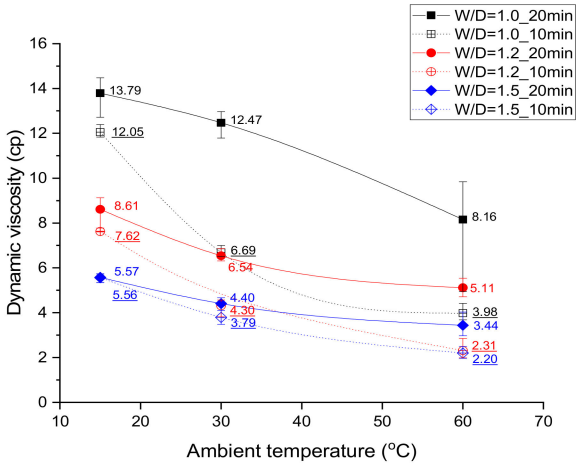

Figure 5. Viscosity changes by mixing time of W:D = 1.0, 1.2, and 1.5 emulsions.

Figure 6 shows the viscosity changes in a W:D = 1.0 emulsion containing 0.2 wt% of mixed surfactant (HLB 14). Viscosity was now independent of mixing time, and about 1.5-fold greater than that without surfactant. Emulsions containing large amounts of water were readily synthesized, but combustion efficiency fell, or combustion was impossible because the proportion of diesel was too low [30]. Thus, the W:D = 1.0 emulsion containing 0.2 wt% of mixed surfactant (HLB 14) was optimal, and was used in the following combustion experiments.

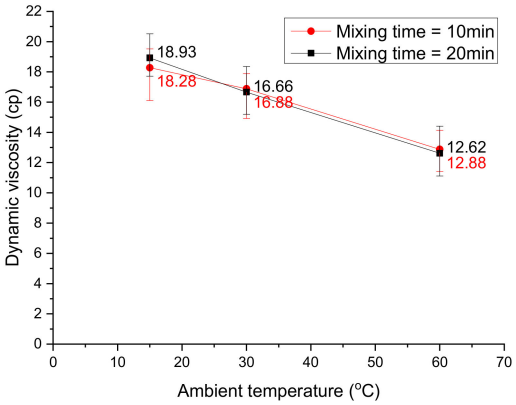

Figure 6. Viscosity changes by mixing time of W:D = 1.0 emulsions containing 0.2 wt% of mixed surfactant (HLB 14).

3.2. Diesel Droplet Combustion

A diesel droplet does not ignite below 700 °C at normal ambient pressure because diesel vapor diffuses rapidly; the vapor/oxygen mixture does not attain the flammability limit [31,32]. Figure 7 shows the temperature variation inside a diesel droplet at various temperatures and pressures. The ignition temperature fell as the ambient temperature rose, because the droplet then evaporated rapidly. After ignition, the droplet temperature increased rapidly because it was heated by the flame (Figure 8). The flame configuration at 1 bar of pressure differed from those of other flames. A diesel droplet was inflated at 1 bar of pressure during fast evaporation because the diesel consists of various components. Ignition is then possible if the fuel/oxygen mixture meets the flammability limit.

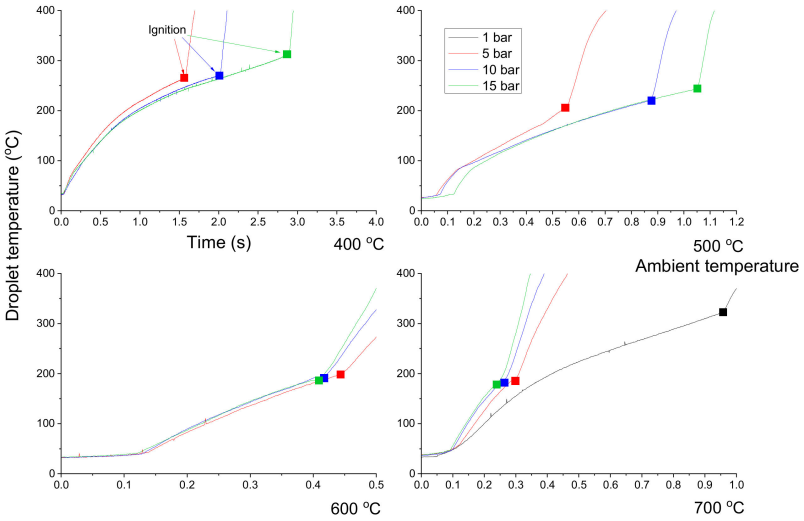

Figure 7. Temperature variation in a diesel droplet at various ambient temperatures and pressure.

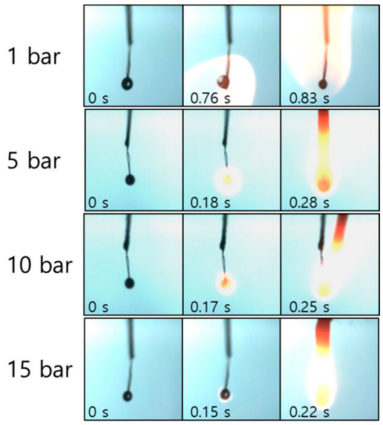

Figure 8. Flame configuration at various ambient pressures and 700 °C.

Figure 9 shows that the ignition delay fell at temperatures below 500 °C as the pressure was reduced, but increased at temperatures over 600 °C. The ignition delay is strongly affected by the evaporation rate, which is proportional to the extent of diffusion and inversely proportional to the latent heat of diesel. The diffusion coefficient decreases as the pressure rises but increases with increasing temperature. The latent heat of diesel decreases as the pressure rises [33]. Thus, the effects are opposite in nature, either enhancing or retarding diesel evaporation; this explains why the trends differ below 500 °C and above 600 °C.

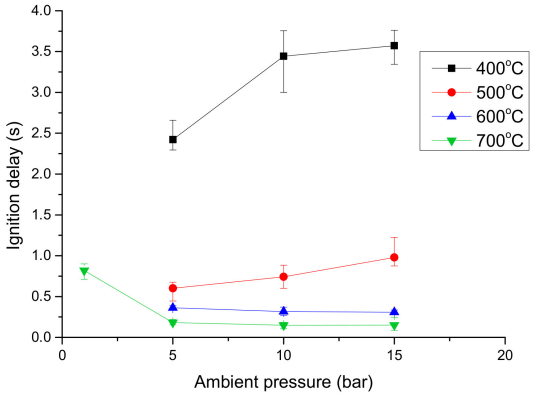

Figure 9. Ignition delay of a diesel droplet at various ambient temperatures and pressures.

The average burning rate was calculated using Equation (2) [22]. The average droplet burning rate is the mean rate of change in the square of the droplet diameter from the time of ignition (*di*) to the time of flame extinction (*df*). The droplet burning time (tburning) is the interval between these time points:

$$K_{b,avg} = \frac{d_i^2 - d_f^2}{t_{burning}} \quad (2)$$

Figure 10 shows that the average burning rate fell as the temperature rose, because the droplet size at the start of ignition was much smaller at 400 than 700 °C, given the long ignition delay. Hence, the average burning rate was relatively high at low temperature. The average burning rate rose with pressure because of heat feedback (Figure 8). Flames lay adjacent to a droplet as the pressure rose; droplet heating thus increased. The average burning rate was abnormally high at 1 bar and 700 °C, because the droplet were inflated by accumulated internal volatile gas prior to ignition.

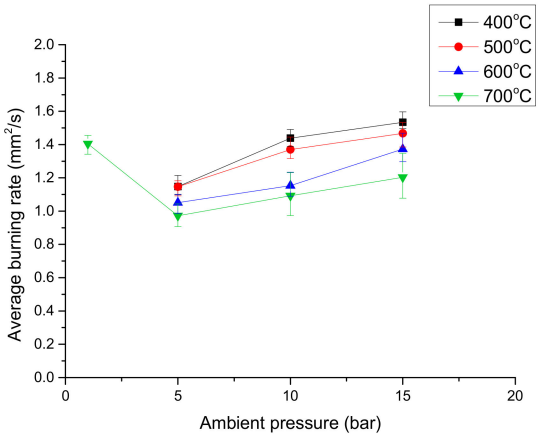

Figure 10. Average burning rate of a diesel droplet at various ambient temperatures and pressures.

3.3. Emulsion Droplet Combustion

Similar to the combustion of diesel droplet, combustion of an emulsion droplet at 1 bar was unable to be observed because of rapid fuel vapor diffusion and strong micro-explosions. Also, the rapid diffusion downgraded mixture quality; the flammability limit was not met, and the micro-explosions detached a droplet from the thermocouple. The micro-explosion of an emulsion droplet reflected the different boiling points of water and diesel. After water vapor accumulated within a droplet, a strong micro-explosion followed as the water jetted out instantaneously. This made it impossible to visualize emulsion droplet combustion at 1 bar and 700 °C.

Figure 11 shows the droplet temperature variations inside an emulsion droplet at various ambient temperatures and pressures. Below an ambient temperature of 500 °C, the ignition point was higher than the water boiling point. During evaporation, the temperature inside the droplet increased to the water boiling point, and did not initially rise any further because of the latent heat of water. Later, the droplet temperature exceeded the water boiling point because some of the heat from ambient gas approaching a droplet was used to evaporate water and heat diesel. Emulsion droplet combustion began at 400 °C after all water had evaporated and the micro-explosion had concluded. However, at an ambient temperature of 500 °C and ambient pressures of 10 or 15 bar, ignition occurred prior to micro-explosion extinction. The ambient pressure suppressed fuel vapor diffusion and the micro-explosion aided mixing; the flow near the droplet increased [22]. Such flow allowed the mixture to attain the flammability limit and rapidly ignite. The flame is shown in Figure 12 and reflects the flow near the droplet and droplet atomization caused by the micro-explosion. High ambient temperature was associated with strong micro-explosions; flaming occurred randomly in the vicinity of a droplet as the temperature rose. During combustion, the temperature within the droplet did not rise because

of the micro-explosion. After all water had evaporated, the flame stabilized, and the temperature then rose further in a uniform manner. Above 600 °C, ignition was rapid as the pressure decreased. Although micro-explosions enhanced ignition at high temperatures, the pressure increase suppressed these explosions.

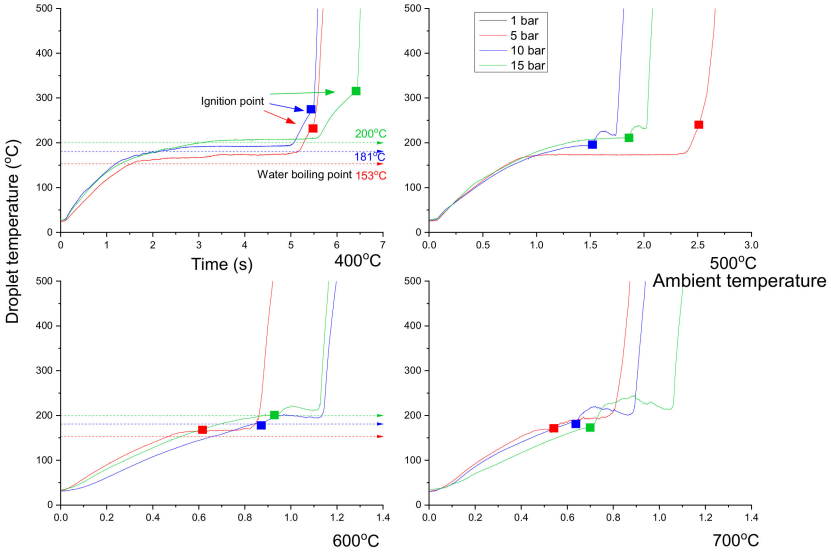

Figure 11. Temperature change in an emulsion droplet at various ambient temperatures and pressures.

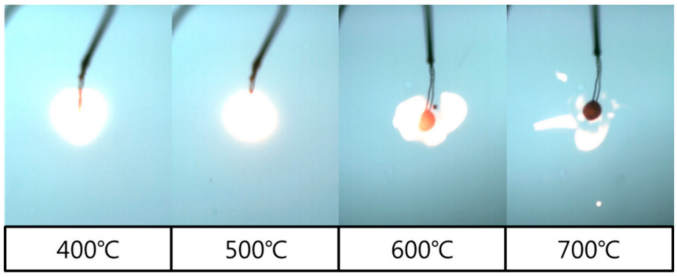

Figure 12. Flame configuration at an emulsion droplet ignition at various ambient temperatures.

Figure 13 shows the emulsion droplet ignition delay at various ambient temperatures and pressures. At 10 bar and below 500 °C, the ignition delay was lowest because the ignition occurred during the micro-explosion. The ignition delay above 600 °C was shorter because micro-explosion actively occurred at lower ambient pressure.

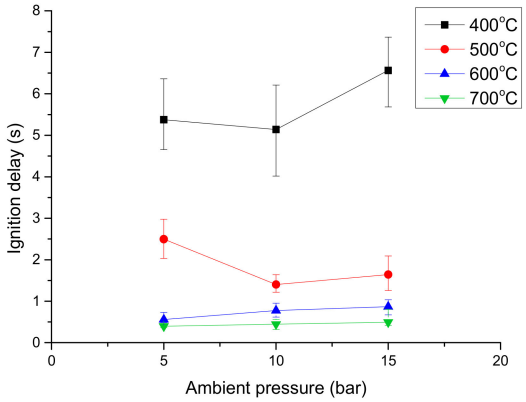

Figure 13. Ignition delay of an emulsion droplet at various ambient temperatures and pressures.

Figure 14 compares the normalized droplet diameter squared of emulsion at 700 °C ambient temperature where do is the initial droplet diameter. As mentioned above, the ignition delay was lowered as lower ambient pressure at 700 °C. The calculated droplet sizes after ignition suddenly changed due to strong micro-explosion because it made the inflated emulsion droplet. Compared to the difference in calculated droplet sizes, the intensity of the strong micro-explosion occurred at low ambient pressure conditions.

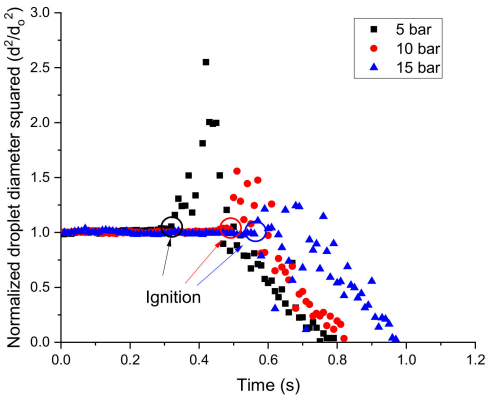

Figure 14. Temporal variation of normalized droplet diameter squared at 700 °C.

3.4. Comparison of the Combustion Behavior of Diesel and Emulsion Fuels

Figure 15 compares total droplet lifetime between the diesel and emulsion fuels; these values are the sum of the ignition delay and flame lifetime (from onset of ignition to flame extinction). The burning rates of emulsion droplet were not uniform because an emulsion droplet was distorted by the micro-explosion. Prior to explosion, water vapor accumulated within the droplet, which thus became inflated, rendering the droplet size random at ignition onset; this explains why the average burning rate of the emulsion droplet was not uniform. Therefore, it was useful to compare total lifetime between the diesel and emulsion droplet. The percentage values are the increases in total emulsion droplet lifetimes compared to those of diesel droplet in Equation (3).

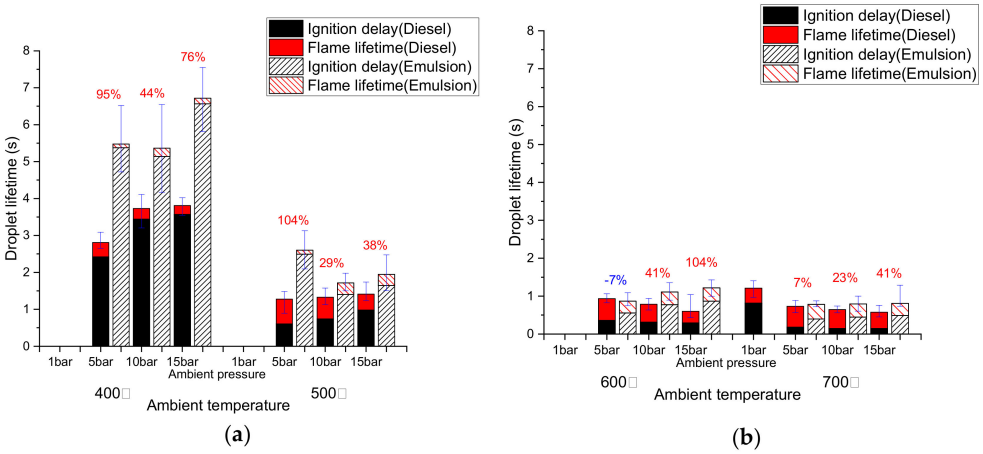

Figure 15. Total diesel and emulsion droplet lifetime (**a**) below 500 °C and (**b**) above 600 °C.

$$\text{Increase rate of emulsion droplet lifetime} = \frac{\text{Emulsion droplet lifetime} - \text{Diesel dorplet lifetime}}{\text{Diesel dorplet lifetime}} \times 100(\%) \quad (3)$$

Figure 15a shows that a diesel droplet exhibited longer total lifetime as the pressure rose, because of ignition delay. This effect predominated at 400 °C but the flame lifetime was similar to that at 500 °C.

However, total emulsion droplet lifetime varied by temperature and pressure; the ignition delay effect always predominated and total droplet lifetime was tightly associated with this delay. As the specific heat of water is about twice that of diesel, and as the micro-explosions hindered ignition, the total emulsion droplet lifetimes were relatively higher than those of diesel droplet under all conditions tested. Figure 15b shows the total droplet lifetime above 600 °C. Under such conditions, the diesel flame lifetime, not the ignition delay, predominated; the total diesel droplet lifetime decreased as the pressure rose due to heat feedback of flame. However, the total emulsion droplet lifetime was still affected by ignition delay, and decreased as micro-explosions became more common with pressure reduction. Under all conditions tested, total emulsion droplet lifetimes were longer than those of diesel droplet, except at 5 bar and 600 °C where the emulsion droplet lifetime was smaller than that of diesel. It occurred because atomized emulsion droplets caused by micro-explosion rapidly burned thus flame lifetime reduced.

4. Conclusions

In this study, various emulsions were synthesized in the range of 0.3 to 1.5 water/diesel mass ratio, and the optimum emulsion-containing surfactant was selected. The auto-ignition and combustion characteristics of a single emulsion droplet, under optimum conditions, were defined at various temperatures and pressures. The results may be summarized as follows:

1. Emulsions formed readily as the water content rose above a 1:1 water:diesel mass ratio. The optimum emulsion fuel was 1:1 water:diesel mass ratio containing 0.2 wt% mixed surfactant (HLB 14) as prepared via 10 min of sonication.
2. The viscosity of the W:D = 1.0 emulsion was the highest because droplet dispersion increased the effective concentration as the shear rate rose. After addition of 0.2 wt% mixed surfactant (HLB 14), the viscosity was independent of mixing time.
3. The ignition delay of a diesel droplet increased below 500 °C as the pressure rose, but decreased at temperatures above 600 °C. However, the ignition delay of an emulsion droplet decreased above 600 °C, as the pressure decreased due to the effect of the micro-explosion.
4. The total lifetime of an emulsion droplet was higher than that of a diesel droplet except under 5 bar, 600 °C condition. Under this condition, the fast flame lifetime of the emulsion droplet represented a shorter total droplet lifetime than diesel.

Based on these results, the viscosity characteristics of emulsion were analyzed and emulsion fuel was found to have the potential to replace diesel.

Author Contributions: Conceptualization, J.W., H.K. and S.W.B; methodology, J.W. and H.K.; Formal analysis, J.W., H.K. and S.W.B.; writing, J.W., H.K., S.W.B. and H.L. All the authors read and confirmed the final manuscript.

Funding: This article was supported by BK21 Plus Program.

Acknowledgments: The English in this document has been checked by at least two professional editors, both native speakers of English. (www.Textcheck.com)

Conflicts of Interest: The authors declare no conflict of interest.

References

1. Selim, M.Y.E.; Ghannam, M.T. Combustion study of stabilized water-in-diesel fuel emulsion. *Energy Sources Part A* **2009**, *32*, 256–274. [CrossRef]
2. Kim, H.M.; Won, J.H.; Baek, S.W. Evaporation of a single emulsion fuel droplet in elevated temperature and pressure conditions. *Fuel* **2018**, *226*, 172–180. [CrossRef]
3. Vellaiyan, S.; Amirthagadeswaran, K.S. Zinc oxide incorporated water-in-diesel emulsion fuel: Formulation, particle size measurement, and emission characteristics assessment. *Pet. Sci. Technol.* **2016**, *34*, 114–122. [CrossRef]

4. Randazzo, M.L.; Sodre, J.R. Exhaust emissions from a diesel powered vehicle fuelled by soybean biodiesel blends (B3–B20) with ethanol as an additive (B20E2–B20E5). *Fuel* **2011**, *90*, 90–103. [CrossRef]
5. Kichatov, B.; Korshunov, A.; Kiverin, A.; Son, E. Experimental study of foamed emulsion combustion: Influence of solid microparticles, glycerol and surfactant. *Fuel Process. Technol.* **2017**, *166*, 77–85. [CrossRef]
6. Avulapati, M.M.; Megaritis, T.; Xia, J.; Ganippa, L. Experimental understanding on the dynamics of micro-explosion and puffing in ternary emulsion droplets. *Fuel* **2019**, *239*, 1284–1292. [CrossRef]
7. Ithnin, A.M.; Ahmad, M.A.; Bakar, M.A.A.; Rajoo, S.; Yahya, W.J. Combustion performance and emission analysis of diesel engine fuelled with water-in-diesel emulsion fuel made from low-grade diesel fuel. *Energy Convers. Manag.* **2015**, *90*, 375–382. [CrossRef]
8. Jang, G.M.; Kim, N.I. Relationships between dynamic behavior and properties of a single droplet of water-emulsified n-dodecane. *Fuel* **2018**, *220*, 130–139. [CrossRef]
9. Elsanusi, O.A.; Roy, M.M.; Sidhu, M.S. Experimental investigation on a diesel engine fueled by diesel-biodiesel blends and their emulsions at various engine operating conditions. *Appl. Energy* **2017**, *203*, 582–593. [CrossRef]
10. Reham, S.S.; Masjuki, H.H.; Kalam, M.A.; Shancita, I.; Fattah, I.M.; Ruhul, A.M. Study on stability, fuel properties, engine combustion, performance and emission characteristics of biofuel emulsion. *Renew. Sustain. Energy Rev.* **2015**, *52*, 1566–1579. [CrossRef]
11. Jeong, I.C.; Lee, K.H. Auto-ignition and micro-explosion behavior of droplet arrays of water-in-fuel emulsion. *Int. J. Automot. Technol.* **2008**, *9*, 735–740. [CrossRef]
12. Ghassemi, H.; Baek, S.W.; Khan, Q.S. Experimental study on evaporation of kerosene droplets at elevated pressures and temperatures. *Combust. Sci. Technol.* **2006**, *178*, 1669–1684. [CrossRef]
13. Ma, Z.; Li, Y.; Li, Z.; Du, W.; Yin, Z.; Xu, Z. Evaporation and combustion characteristics of hydrocarbon fuel droplet in sub- and super-critical environments. *Fuel* **2018**, *220*, 763–768. [CrossRef]
14. Faik, A.; Zhang, Y. Multicomponent fuel droplet combustion investigation using magnified high speed backlighting and shadowgraph imaging. *Fuel* **2018**, *221*, 89–109. [CrossRef]
15. Zhang, X.; Li, T.; Wang, B.; Wei, Y. Superheat limit and micro-explosion in droplets of hydrous ethanol-diesel emulsions at atmospheric pressure and diesel-like conditions. *Energy* **2018**, *154*, 535–543. [CrossRef]
16. Genot, C.; Kabri, T.H.; Meynier, A. Stabilization of omega-3 oils and enriched foods using emulsifiers. In *Food Enrichment with Omega-3 Fatty Acids*; Woodhead Publishing: Sawston, Cambridge, UK, 2013; pp. 150–193.
17. Noor El-Din, M.R.; El-Hamouly, S.H.; Mohamed, H.M.; Mishrif, M.R.; Ragab, A.M. Water-in diesel fuel nanoemulsions: Preparation, stability, and physical properties. *Egypt. J. Pet.* **2013**, *22*, 517–530. [CrossRef]
18. Xie, F.; Brooks, B.W. Phase behaviour of a non-ionic surfactant-polymeric solution-water system during the phase inversion process. *Colloids Surf. A Physicochem. Eng. Asp.* **2005**, *252*, 27–32. [CrossRef]
19. Liang, X.; Wu, J.; Yang, X.; Tu, Z.; Wang, Y. Investigation of oil-in-water emulsion stability with relevant interfacial characteristics simulated by dissipative particles dynamics. *Colloids Surf. A Physicochem. Eng. Asp.* **2018**, *546*, 107–114. [CrossRef]
20. Rastogi, P.; Mehta, P.S.; Kaisare, N.S.; Basavaraj, M.G. Kinetic stability of surfactant stabilized water-in-diesel emulsion fuels. *Fuel* **2019**, *236*, 1415–1422.
21. Fan, X.; Hu, W.; Yang, J.; Xu, X.; Gao, J. A New emulsifier behavior of the preparation for micro-emulsified diesel oil. *Pet. Sci. Technol.* **2008**, *26*, 2125–2136. [CrossRef]
22. Won, J.H.; Baek, S.W.; Kim, H.M. Autoignition and combustion behavior of emulsion droplet under elevated temperature and pressure conditions. *Energy* **2018**, *163*, 800–810. [CrossRef]
23. Harada, T.; Watanabe, H.; Suzuki, Y.; Kamata, H.; Matsushita, Y.; Aoki, H.; Miura, T. A numerical investigation of evaporation characteristics of a fuel droplet suspended from a thermocouple. *Int. J. Heat Mass Transf.* **2011**, *54*, 649–655. [CrossRef]
24. Khan, Q.S.; Baek, S.W.; Ghassemi, H. On the autoignition and combustion characteristics of kerosene droplets at elevated pressure and temperature. *Combust. Sci. Technol.* **2007**, *179*, 2437–2451. [CrossRef]
25. Kim, H.M.; Baek, S.W.; Chang, D.J. Auto-ignition characteristics of single n-heptane droplet in a rapid compression machine. *Combust. Sci. Technol.* **2014**, *186*, 912–927. [CrossRef]
26. Joshi, R.M.; Pegg, M.J. Flow properties of biodiesel fuel blends at low temperatures. *Fuel* **2007**, *86*, 143–151. [CrossRef]
27. The Engineering ToolBox. Available online: https://www.engineeringtoolbox.com/water-dynamic-kinematic-viscosity-d_596.html (accessed on 12 February 2019).

28. Benayoune, M.; Khezzar, L.; Al-Rumhy, M. Viscosity of water in oil emulsions. *Pet. Sci. Technol.* **1998**, *16*, 767–784. [CrossRef]
29. Singh, B.P.; Pandey, B.P. Ultrasonication for breaking water-in-oil emulsions. *Proc. Indian Natl. Sci. Acad. USA* **1992**, *58*, 181–194.
30. Antonov, V.N. Features of preparation of water-fuel emulsions for diesel engines. *Chem. Technol. Fuels Oils* **1983**, *19*, 606–609. [CrossRef]
31. Javed, I.; Baek, S.W. Autoignition and combustion characteristics of kerosene droplets with dilute concentrations of aluminum nanoparticles at elevated temperatures. *Combust. Flame* **2015**, *162*, 774–787. [CrossRef]
32. Lee, D.G.; Won, J.H.; Kim, H.M.; Baek, S.W. Autoignition behavior of an ethanol-methylcellulose gel droplet in a hot environment. *Energies* **2018**, *11*, 2168. [CrossRef]
33. Turns, S.R. *An Introduction to Combustion: Concepts and Applications*, 2nd ed.; McGraw-Hill: Singapore, 2005; pp. 337–394.